

Time-space Finite Element Adaptive AMG for Multi-term Time Fractional Advection Diffusion Equations

Xiaoqiang Yue^{a,b}, Yehong Xu^a, Shi Shu^{b,*}, Menghuan Liu^a, Weiping Bu^b

^a*School of Mathematics and Computational Science, Xiangtan University, Hunan 411105, P.R. China*

^b*Hunan Key Laboratory for Computation and Simulation in Science and Engineering, Xiangtan University, Hunan 411105, P.R. China*

Abstract

In this study we construct a time-space finite element (FE) scheme and furnish cost-efficient approximations for one-dimensional multi-term time fractional advection diffusion equations on a bounded domain Ω . Firstly, a fully discrete scheme is obtained by the linear FE method in both temporal and spatial directions, and many characterizations on the resulting matrix are established. Secondly, the condition number estimation is proved, an adaptive algebraic multigrid (AMG) method is further developed to lessen computational cost and analyzed in the classical framework. Finally, some numerical experiments are implemented to reach the saturation error order in the $L^2(\Omega)$ norm sense, and present theoretical confirmations and predictable behaviors of the proposed algorithm.

Keywords: Multi-term time fractional advection diffusion equations, time-space finite element, condition number estimation, algorithmic complexity, adaptive AMG method

2010 MSC: 35R11, 65F10, 65F15, 65N55

1. Introduction

In recent years, fractional differential equations (FDEs) have burst onto the scientific computing scene as a powerful instrument in descriptions of memory and hereditary that has yielded a wide variety of applications in physics, hydrology, finance and other fields [1]. Since the vast majority
 5 couldn't be solved accurately, or their analytical solutions (if luckily derived) always contain specific infinite series resulting in sharp costs of evaluations, numerical solutions to FDEs becomes very practical and prevalent. Numerous numerical (unconditionally stable and efficient) methods arise,

*Corresponding author

Email addresses: yuexq@xtu.edu.cn (Xiaoqiang Yue), shushi@xtu.edu.cn (Shi Shu)

e.g. finite difference (FD) [2–6], finite element (FE) [7–13], finite volume [14] and spectral (element) methods [15–18].

Fractional advection diffusion equations (FADEs) are known as one of the foremost models in depictions for transport process in complex systems governed by the abnormal diffusion and non-exponential relaxation patterns [19]. Fundamental and numerical solutions for FADEs with single-term, two-term and multi-term time fractional derivatives have been investigated in [7, 20–26]. Nonetheless, from the survey of references, there are no calculations regarding the time-space FE discretization for FADEs in literature. In this paper we focus on this topic to the one-dimensional version of multi-term time fractional advection diffusion equations (MTFADEs)

$$\sum_{i=0}^s a_i {}^C D_t^{\alpha_i} u(x, t) = K_1 \frac{\partial^{2\beta} u(x, t)}{\partial |x|^{2\beta}} + K_2 \frac{\partial^{2\gamma} u(x, t)}{\partial |x|^{2\gamma}} + f(x, t), \quad t \in I = (0, T], \quad x \in \Omega = (a, b) \quad (1)$$

$$u(a, t) = u(b, t) = 0, \quad t \in I \quad (2)$$

$$u(x, 0) = \psi_0(x), \quad x \in \bar{\Omega} \quad (3)$$

10 with orders $0 < \alpha_s < \dots < \alpha_1 < \alpha_0 < 1$, $\beta \in (0, 1/2)$ and $\gamma \in (1/2, 1)$, constants $a_0 > 0$, $a_i \geq 0$ ($i = 1, \dots, s$), $K_1 > 0$ and $K_2 > 0$, Caputo of order α ($0 < \alpha < 1$) and Riesz of order 2ϱ ($m - 1 < 2\varrho < m$) fractional derivatives defined by

$${}^C D_t^\alpha u = \frac{1}{\Gamma(1 - \alpha)} \int_0^t (t - s)^{-\alpha} \frac{\partial u}{\partial s} ds, \quad \frac{\partial^{2\varrho} u}{\partial |x|^{2\varrho}} = -\frac{1}{2 \cos(\varrho\pi)} ({}_x D_L^{2\varrho} u + {}_x D_R^{2\varrho} u)$$

respectively, where

$${}_x D_L^{2\varrho} u = \frac{1}{\Gamma(m - 2\varrho)} \frac{\partial^m}{\partial x^m} \int_a^x (x - s)^{m-1-2\varrho} u ds, \quad {}_x D_R^{2\varrho} u = \frac{(-1)^m}{\Gamma(m - 2\varrho)} \frac{\partial^m}{\partial x^m} \int_x^b (s - x)^{m-1-2\varrho} u ds.$$

Another important note is that no matter which fully discrete scheme is utilized, there always
 15 exists the computational challenge in nonlocality caused by fractional differential operators [27]. Quite many scholars are working to identify algorithms most appropriate to overcome the challenge and utilize computer resources. Multigrid exploits a hierarchy of grids or multiscale representations, and reduces the error of the approximation at a number of frequencies (from global smooth to local oscillation) simultaneously [28–31], which makes multigrid as an extremely superior solver or
 20 preconditioner of particular interest. Pang and Sun presented an efficient V-cycle geometric multi-grid (GMG) with fast Fourier transform (FFT) to solve one-dimensional space-fractional diffusion equations (SFDEs) discretized by an implicit FD scheme [32]. Bu et al. extended and analyzed the V-cycle GMG for one-dimensional MTFADs via the FD in temporal and FE in spatial directions [26]. Zhou and Wu discussed the FE F-cycle GMG to linear stationary FADEs in Riemann-Liouville

fractional derivatives [33]. Jiang and Xu constructed optimal GMG approaches for two-dimensional SFDEs to get FE approximations [34]. Chen et al. generalized an algebraic multigrid (AMG) with line smoothers to fractional Laplacian problems through localizing them as nonuniform elliptic equations [35]. Zhao et al. considered the adaptive FE V-cycle GMG for one-dimensional SFDEs using hierarchical matrices [36]. Chen and Deng exploited GMG's coarsening strategy and grid-transfer operators, equipped with Galerkin coarse-grid operator to produce a robust multigrid but with much lower convergence rate for nonlocal models with a finite range of interactions [37]. More recently, we developed and analyzed a straightforward adaptive AMG through condition number estimations for one-dimensional time-space Caputo-Riesz FDEs [38]. To the best of our knowledge, cost-efficient AMG resolutions for MTFADEs by fully time-space FE schemes are still limited.

The goal of this paper is to design a time-space FE scheme and develop a fairly robust and efficient solver for problem (1)-(3). The remainder proceeds as follows. Section 2 contains a review of preliminary knowledge on fractional derivative spaces, covers the constitution and fundamental properties of the fully discrete FE discretization. In section 3, condition number estimation on the coefficient matrix is discussed, followed by the construction and convergence analysis of an adaptive AMG method. Section 4 reports and analyzes numerical results to showcase the benefits, and some concluding remarks with follow-up work are given in section 5.

For simplicity, symbols \lesssim , \gtrsim and \simeq are used throughout the paper: $u_1 \lesssim v_1$ symbolizes $u_1 \leq C_1 v_1$, $u_2 \gtrsim v_2$ means $u_2 \geq c_2 v_2$ while $u_3 \simeq v_3$ stands for $c_3 v_3 \leq u_3 \leq C_3 v_3$, where C_1 , c_2 , c_3 and C_3 are positive constants independent of step sizes and variables.

2. Time-space FE scheme for MTFADEs

In this section we will briefly draw some fractional derivative spaces and several relevant auxiliary results, which is the basis of our description of the time-space FE scheme in section 2.2, where also address numerous features of the resulting stiffness and coefficient matrices.

2.1. Reminder on fractional calculus

Definition 1. (Left and right fractional derivative spaces) For any constant $\mu > 0$, define norms

$$\|u\|_{J_L^\mu(\Omega)} := (\|u\|_{L^2(\Omega)}^2 + \|{}_x D_L^\mu u\|_{L^2(\Omega)}^2)^{\frac{1}{2}}, \quad \|u\|_{J_R^\mu(\Omega)} := (\|u\|_{L^2(\Omega)}^2 + \|{}_x D_R^\mu u\|_{L^2(\Omega)}^2)^{\frac{1}{2}},$$

and let $J_{L,0}^\mu(\Omega)$ and $J_{R,0}^\mu(\Omega)$ be closures of $C_0^\infty(\Omega)$ under $\|\cdot\|_{J_L^\mu(\Omega)}$ and $\|\cdot\|_{J_R^\mu(\Omega)}$, respectively.

Definition 2. (Fractional Sobolev space) For any constant $\mu > 0$, define the norm

$$\|u\|_{H^\mu(\Omega)} := (\|u\|_{L^2(\Omega)}^2 + \|\xi|^\mu \tilde{u}\|_{L^2(\Omega_\xi)}^2)^{\frac{1}{2}},$$

and let $H_0^\mu(\Omega)$ be the closure of $C_0^\infty(\Omega)$ in $\|\cdot\|_{H^\mu(\Omega)}$ sense, where \tilde{u} is the Fourier transform of u .

Lemma 1. (see [8], Proposition 1) If constant $\mu \in (0, 1)$ and $u, v \in J_{L,0}^{2\mu}(\Omega)$ (or $J_{R,0}^{2\mu}(\Omega)$), then

$$({}_x D_L^{2\mu} u, v)_{L^2(\Omega)} = ({}_x D_L^\mu u, {}_x D_R^\mu v)_{L^2(\Omega)}, \quad ({}_x D_R^{2\mu} u, v)_{L^2(\Omega)} = ({}_x D_R^\mu u, {}_x D_L^\mu v)_{L^2(\Omega)}.$$

55 **Lemma 2.** (see [7], Lemma 2.4) For any constant $\mu > 0$ and real valued function u , we have

$$({}_x D_L^\mu u, {}_x D_R^\mu u)_{L^2(\Omega)} = \cos(\pi\mu) \|{}_x D_L^\mu u\|_{L^2(\Omega)}^2.$$

Lemma 3. (Fractional Poincaré-Friedrichs, see [7], Theorem 2.10) Let $\mu > 0$. For $u \in J_{L,0}^\mu(\Omega)$, we have

$$\|u\|_{L^2(\Omega)} \lesssim \|{}_x D_L^\mu u\|_{L^2(\Omega)}.$$

2.2. Derivation and characterizations of the time-space FE scheme

Utilizing Lemma 1, referring to (1), we can derive the variational formulation: given $\psi_0 \in L^2(\Omega)$, $f \in L^2(\Omega, I)$ and $Q_t := \Omega \times (0, t)$, to find $u \in \mathcal{H} := H_0^\gamma(\Omega) \times H^1(I)$ subject to $u(x, 0) = \psi_0(x)$ as well as

$$\sum_{i=0}^s a_i ({}_0^C D_\sigma^{\alpha_i} u, v)_{Q_t} + B_\Omega^t(u, v) = (f, v)_{Q_t}, \quad \forall v \in \mathcal{H}^* := H_0^\gamma(\Omega) \times L^2(I), \quad (4)$$

where $({}_0^C D_\sigma^{\alpha_i} u, v)_{Q_t} = \int_0^t ({}_0^C D_\sigma^{\alpha_i} u, v)_{L^2(\Omega)} d\sigma$, $(f, v)_{Q_t} = \int_0^t (f, v)_{L^2(\Omega)} d\sigma$ and

$$B_\Omega^t(u, v) = \int_0^t \frac{K_1}{2 \cos(\beta\pi)} [({}_x D_L^\beta u, {}_x D_R^\beta v)_{L^2(\Omega)} + ({}_x D_R^\beta u, {}_x D_L^\beta v)_{L^2(\Omega)}] d\sigma + \int_0^t \frac{K_2}{2 \cos(\gamma\pi)} [({}_x D_L^\gamma u, {}_x D_R^\gamma v)_{L^2(\Omega)} + ({}_x D_R^\gamma u, {}_x D_L^\gamma v)_{L^2(\Omega)}] d\sigma.$$

To give a description of our time-space FE scheme, we firstly make a temporal mesh $0 = t_0 <$
60 $t_1 < \dots < t_N = T$ and a uniform spatial discretization of the interval $\bar{\Omega}$ by points $x_i = a + ih$ ($i = 0, 1, \dots, M$) with constant spacing $h = (b - a)/M$. We set

$$I_j = (t_{j-1}, t_j), \quad \tilde{I}_j = (0, t_j), \quad \tau_j = t_j - t_{j-1}, \quad j = 1, 2, \dots, N; \quad \Omega_h = \{\Omega_l = (x_{l-1}, x_l) : l = 1, 2, \dots, M\}.$$

Next, we introduce the FE spaces in tensor products

$$\mathcal{V}_n = \mathcal{V}_h^\gamma(\Omega_h) \times \mathcal{V}_\tau(\tilde{I}_n), \quad \mathcal{V}_n^* = \mathcal{V}_h^\gamma(\Omega_h) \times \mathcal{V}_\tau^*(I_n),$$

where $\mathcal{V}_h^\gamma(\Omega_h) = \{w_h \in H_0^\gamma(\Omega) \cap C(\bar{\Omega}) : w_h(x)|_{\Omega_l} \in \mathcal{P}_1(\Omega_l), l = 1, \dots, M\}$, $\mathcal{V}_\tau(\tilde{I}_n) = \{v_\tau \in \mathcal{C}(\tilde{I}_n) : v_\tau(0) = 1, v_\tau(t)|_{I_j} \in \mathcal{P}_1(I_j), j = 1, \dots, n\}$ and $\mathcal{V}_\tau^*(I_n) = \{v_\tau \in L^2(I_n) : v_\tau(t)|_{I_n} \in \mathcal{P}_0(I_n)\}$. Here

65 \mathcal{P}_k denotes the space of all polynomials of degree $\leq k$.

We now get ready to define the time-space FE numerical scheme of problem (4): for $Q_n := \Omega_h \times I_n$, find $u_{h\tau} \in \mathcal{V}_n$ such that

$$\sum_{i=0}^s a_i ({}^C D_t^{\alpha_i} u_{h\tau}, v_{h\tau})_{Q_n} + B_\Omega^n(u_{h\tau}, v_{h\tau}) = (f, v_{h\tau})_{Q_n}, \quad \forall v_{h\tau} \in \mathcal{V}_n^* \quad (5)$$

along with $u_{h\tau}(x, 0) = \psi_{0,I}(x)$, where $\psi_{0,I}(x) \in \mathcal{V}_n$ satisfies $\psi_{0,I}(x_i) = \psi_0(x_i)$ ($i = 0, 1, \dots, M$),

$$({}^C D_t^{\alpha_i} u_{h\tau}, v_{h\tau})_{Q_n} = \int_{t_{n-1}}^{t_n} ({}^C D_t^{\alpha_i} u_{h\tau}, v_{h\tau})_{L^2(\Omega)} dt, \quad (f, v_{h\tau})_{Q_n} = \int_{t_{n-1}}^{t_n} (f, v_{h\tau})_{L^2(\Omega)} dt$$

and

$$B_\Omega^n(u_{h\tau}, v_{h\tau}) = \int_{t_{n-1}}^{t_n} \frac{K_1}{2 \cos(\beta\pi)} [({}_x D_L^\beta u_{h\tau}, {}_x D_R^\beta v_{h\tau})_{L^2(\Omega)} + ({}_x D_R^\beta u_{h\tau}, {}_x D_L^\beta v_{h\tau})_{L^2(\Omega)}] dt + \int_{t_{n-1}}^{t_n} \frac{K_2}{2 \cos(\gamma\pi)} [({}_x D_L^\gamma u_{h\tau}, {}_x D_R^\gamma v_{h\tau})_{L^2(\Omega)} + ({}_x D_R^\gamma u_{h\tau}, {}_x D_L^\gamma v_{h\tau})_{L^2(\Omega)}] dt.$$

To go a little further, let

$$\mathcal{L}_0(t) = \begin{cases} \frac{t_1 - t}{\tau_1}, & t \in I_1 \\ 0, & t \in \tilde{I}_n \setminus I_1 \end{cases}, \quad \mathcal{L}_k(t) = \begin{cases} \frac{t_{k+1} - t}{\tau_{k+1}}, & t \in I_{k+1} \\ \frac{t - t_{k-1}}{\tau_k}, & t \in I_k \\ 0, & t \in \tilde{I}_n \setminus (I_k \cup I_{k+1}) \end{cases}, \quad \mathcal{L}_n(t) = \begin{cases} \frac{t - t_{n-1}}{\tau_n}, & t \in I_n \\ 0, & t \in \tilde{I}_n \setminus I_n \end{cases}$$

70 and

$$\tilde{\mathcal{L}}_0^i(t) = \frac{\int_{t_0}^{\hat{t}_1} (t-s)^{-\alpha_i} d\mathcal{L}_0(s)}{\Gamma(1-\alpha_i)}, \quad \tilde{\mathcal{L}}_k^i(t) = \frac{\int_{t_{k-1}}^{\hat{t}_{k+1}} (t-s)^{-\alpha_i} d\mathcal{L}_k(s)}{\Gamma(1-\alpha_i)}, \quad \tilde{\mathcal{L}}_n^i(t) = \frac{\int_{t_{n-1}}^t (t-s)^{-\alpha_i} d\mathcal{L}_n(s)}{\Gamma(1-\alpha_i)}$$

with $\hat{t}_j = \min(t, t_j)$ for $j = 1, \dots, n$ and $k = 1, \dots, n-1$.

Note that, in view of (2), the definition of \mathcal{V}_n^* leads to the relation

$$\mathcal{V}_n^* = \text{span}\{\phi_l(x) \times 1, l = 1, \dots, M-1\},$$

where $\phi_l(x)$ plays the role of the so-called shape function at point x_l . For the monolithic representation $u_{h\tau}(x, t) = \sum_{k=0}^n u_h^k(x) \mathcal{L}_k(t)$, by direct calculations and taking

$$({}_x D_L^\mu \phi_i, {}_x D_R^\mu \phi_j)_{L^2(\Omega)} = -({}_x D_L^{2\mu-1} \phi_i, \frac{d\phi_j}{dx})_{L^2(\Omega)}, \quad \mu = \beta, \gamma$$

and the stiffness matrices $A_h^\mu = (a_{i,j}^{\mu,h})_{(M-1) \times (M-1)}$ ($\mu = \beta, \gamma$) with each entry of the same form

$$\begin{cases} a_{i,i}^{\mu,h} = \frac{h^{1-2\mu}(2^{4-2\mu} - 8)}{2 \cos(\mu\pi)\Gamma(4-2\mu)}, & i = 1, \dots, M-1 \\ a_{j,j+1}^{\mu,h} = a_{j+1,j}^{\mu,h} = \frac{h^{1-2\mu}(3^{3-2\mu} - 2^{5-2\mu} + 7)}{2 \cos(\mu\pi)\Gamma(4-2\mu)}, & j = 1, \dots, M-2 \\ a_{k,k+l}^{\mu,h} = a_{k+l,k}^{\mu,h} = \frac{h^{1-2\mu}}{2 \cos(\mu\pi)\Gamma(4-2\mu)} [(l+2)^{3-2\mu} \\ - 4(l+1)^{3-2\mu} + 6l^{3-2\mu} - 4(l-1)^{3-2\mu} + (l-2)^{3-2\mu}], & k = 1, \dots, M-l-1 \end{cases} \quad (9)$$

80 **Remark 1.** The equation (6) follows via multiplying both members of (5) by $\Gamma(3-\alpha_0)\tau_n^{\alpha_0-1}$, for the purpose of preventions on severe losses in accuracy and convergence of the time-space FE scheme.

An important property on the coefficient matrix $\mathcal{A}_{h\tau}^n$ by (7) is stated in the under-mentioned lemma, as a natural consequence of the symmetric Toeplitz-like structures of matrices M_h by (8), A_h^β and A_h^γ by (9).

85 **Lemma 4.** $\mathcal{A}_{h\tau}^n$ is a symmetric Toeplitz matrix. Moreover, it is independent of the temporal level n when the time discretization mesh is uniformly spaced.

Remark 2. Lemma 4 implies that (i) a requirement of only $\mathcal{O}(M)$ is used to store $\mathcal{A}_{h\tau}^n$, (ii) FFT is the most natural choice for matrix-vector multiplications to take advantage of the Toeplitz structure in $\mathcal{O}(M \log M)$ computational complexity.

90 Some important properties of A_h^γ , the stiffness matrix regarding the diffusion term of (1), have been already established in [38], which are stated below.

Lemma 5. (see [38], Theorem 1) The stiffness matrix A_h^γ satisfies

1. $a_{i,i}^{\gamma,h} > 0$ for $i = 1, \dots, M-1$;
2. $a_{i,j}^{\gamma,h} < 0$ for $i \neq j, i, j = 1, \dots, M-1$;
- 95 3. $\sum_{j=1}^{M-1} a_{i,j}^{\gamma,h} > 0$ for $i = 1, \dots, M-1$.

As a result, A_h^γ is an M -matrix. Moreover, for the particular case when $h \leq 1/7$, we have

$$\sum_{j=1}^{M-1} a_{i,j}^{\gamma,h} \geq \begin{cases} -\frac{h^{1-2\gamma}(4-2^{3-2\gamma})}{2 \cos(\gamma\pi)\Gamma(4-2\gamma)}, & i = 1, M-1 \\ -\frac{2^{2\gamma}h(2\gamma-1)}{\cos(\gamma\pi)\Gamma(2-2\gamma)}, & i = 2, \dots, M-2 \end{cases} \quad (10)$$

Now, a few characterizations on A_h^β , the stiffness matrix from the advection term in (1), can be also obtained with some important differences. At this point we denote by β_0 the unique root of the equation $3^{3-2\beta} - 2^{5-2\beta} + 7 = 0$ in the interval $(0, 1/2)$.

Theorem 1. *The stiffness matrix A_h^β holds the following properties.*

1. $a_{i,i}^{\beta,h} > 0$ for $i = 1, \dots, M-1$;
2. If $\beta > \beta_0$, then $a_{i,j}^{\beta,h} < 0$ for $i \neq j$, $i, j = 1, \dots, M-1$;
Else $a_{k,k+1}^{\beta,h} = a_{k+1,k}^{\beta,h} \geq 0$ for $k = 1, \dots, M-2$ and $a_{i,j}^{\beta,h} < 0$ for $|i-j| > 1$, $i, j = 1, \dots, M-1$;
3. $\sum_{j=1}^{M-1} a_{i,j}^{\beta,h} > 0$ for $i = 1, \dots, M-1$.

Thus A_h^β is an M-matrix if and only if $\beta \geq \beta_0$. Moreover, for the particular case when $h \leq 1/7$, we have

$$\sum_{j=1}^{M-1} a_{i,j}^{\beta,h} \geq \begin{cases} -\frac{h^{1-2\beta}(4-2^{3-2\beta})}{2\cos(\beta\pi)\Gamma(4-2\beta)}, & i = 1, M-1 \\ -\frac{2^{2\beta}h(2\beta-1)}{\cos(\beta\pi)\Gamma(2-2\beta)}, & i = 2, \dots, M-2 \end{cases}. \quad (11)$$

Proof. Property 1 follows immediately since $4-2\beta \in (3, 4)$ and $\cos(\beta\pi) > 0$. It is clear that if $\beta > \beta_0$, then $3^{3-2\beta} - 2^{5-2\beta} + 7 < 0$, which gives $a_{j,j+1}^{\beta,h} = a_{j+1,j}^{\beta,h} < 0$ for $j = 1, \dots, M-2$; Otherwise $a_{j,j+1}^{\beta,h} = a_{j+1,j}^{\beta,h} \geq 0$ for $j = 1, \dots, M-2$. The rest of the property 2 is equivalent to the condition

$$f_\beta(l) = (l+2)^{3-2\beta} - 4(l+1)^{3-2\beta} + 6l^{3-2\beta} - 4(l-1)^{3-2\beta} + (l-2)^{3-2\beta} < 0 \quad (12)$$

for $2 \leq l \leq M-2$. Hereafter we assume that $\Omega = (0, 1)$ without loss of generality. By making use of Taylor's expansion with $x_l = lh$, yields

$$f_\beta(l) = h^{1+2\beta}(3-2\beta)(2-2\beta)(1-2\beta)(-2\beta) \left[x_l^{-1-2\beta} + \frac{h(-2\beta-1)}{5!}(-4x_{\xi_1}^{-2-2\beta} + 4x_{\xi_2}^{-2-2\beta} + 32x_{\xi_3}^{-2-2\beta} - 32x_{\xi_4}^{-2-2\beta}) \right], \quad x_{\xi_1} \in (x_l, x_{l+1}), \quad x_{\xi_2} \in (x_{l-1}, x_l), \quad x_{\xi_3} \in (x_l, x_{l+2}), \quad x_{\xi_4} \in (x_{l-2}, x_l).$$

We note that the inequality

$$x_l^{-1-2\beta} + \frac{h(2\beta+1)}{5!}(4x_{l+1}^{-2-2\beta} - 4x_{l-1}^{-2-2\beta} - 32x_l^{-2-2\beta} + 32x_l^{-2-2\beta}) = h^{-1-2\beta} \left\{ l^{-1-2\beta} + \frac{4(2\beta+1)}{5!} \left[(l+1)^{-2-2\beta} - (l-1)^{-2-2\beta} \right] \right\} > 0$$

is clearly true because of the simple observation that the inequality

$$\left(\frac{l}{l+1}\right)^{2+2\beta} - \left(\frac{l}{l-1}\right)^{2+2\beta} > -\frac{l \times 5!}{4(2\beta+1)}$$

holds for $2 \leq l \leq M - 2$. This gives a derivation of (12).

To prove the property 3, it is sufficient to validate

$$\left({}_x D_L^{2\beta-1} \tilde{\phi}, \frac{d\phi_i}{dx} \right)_{L^2(\Omega)} + \left({}_x D_L^{2\beta-1} \phi_i, \frac{d\tilde{\phi}}{dx} \right)_{L^2(\Omega)} < 0, \quad i = 1, \dots, M-1,$$

110 where $\tilde{\phi} := \sum_{j=1}^{M-1} \phi_j = 1 - \phi_0 - \phi_M$. More precisely,

$$\frac{1}{h} \left[\left({}_x D_L^{2\beta-1} \tilde{\phi}, 1 \right)_{L^2(\Omega_i)} - \left({}_x D_L^{2\beta-1} \tilde{\phi}, 1 \right)_{L^2(\Omega_{i+1})} + \left({}_x D_L^{2\beta-1} \phi_i, 1 \right)_{L^2(\Omega_1)} - \left({}_x D_L^{2\beta-1} \phi_i, 1 \right)_{L^2(\Omega_M)} \right] < 0.$$

Let $\varsigma = 3 - 2\beta \in (2, 3)$ for short. For the cases $i = 1$ and $i = M - 1$, by Taylor's formula, we have to prove

$$\begin{aligned} \hat{f}_\varsigma(i) := & \frac{1}{h^2 \Gamma(\varsigma + 1)} \left\{ (4 - 2^\varsigma) h^\varsigma - \varsigma(\varsigma - 1)(\varsigma - 2) h^3 + \frac{3\varsigma(\varsigma - 1)(\varsigma - 2)(\varsigma - 3)}{4!} h^4 \times \right. \\ & \left. \left[(1 - \xi_1)^{\varsigma-4} - 16(1 - \xi_2)^{\varsigma-4} + 27(1 - \xi_3)^{\varsigma-4} \right] \right\} < 0, \quad \xi_1 \in (0, h), \quad \xi_2 \in (0, 2h), \quad \xi_3 \in (0, 3h), \end{aligned}$$

which is an immediate consequence of the relation

$$\frac{(2^\varsigma - 4)h^\varsigma}{\varsigma(\varsigma - 1)(\varsigma - 2)h^3} > \frac{(\varsigma - 3)h}{8} [28 - 16(1 - 2h)^{\varsigma-4}] - 1.$$

On the other hand, all that is needed is the inequality

$$\begin{aligned} \tilde{f}_\varsigma(i) := & \frac{1}{h^2 \Gamma(\varsigma + 1)} \left\{ 3(ih)^\varsigma - 3[(i-1)h]^\varsigma + [(i-2)h]^\varsigma - [(i+1)h]^\varsigma \right. \\ & \left. + 3(1-ih)^\varsigma - [1 - (i-1)h]^\varsigma - 3[1 - (i+1)h]^\varsigma + [1 - (i+2)h]^\varsigma \right\} < 0. \end{aligned} \quad (13)$$

In fact, using 6-order Taylor series expansion, it can be easily shown that the inequality

$$3(ih)^\varsigma - 3[(i-1)h]^\varsigma + [(i-2)h]^\varsigma - [(i+1)h]^\varsigma < -h^3 \varsigma(\varsigma - 1)(\varsigma - 2) x_i^{\varsigma-3}$$

follows by observing that

$$\left(\frac{i-1}{i} \right)^{6-\varsigma} > \frac{12(5-\varsigma)}{252(5-\varsigma) + i \times 6!}, \quad i = 2, \dots, M-2.$$

One further can similarly derive

$$3(1-ih)^\varsigma - [1 - (i-1)h]^\varsigma - 3[1 - (i+1)h]^\varsigma + [1 - (i+2)h]^\varsigma < -h^3 \varsigma(\varsigma - 1)(\varsigma - 2)(1-x_i)^{\varsigma-3}.$$

115 Thus, combining the fact that $x_i^{\varsigma-3} + (1-x_i)^{\varsigma-3} \geq 2^{4-\varsigma}$ for any $x_i \in (0, 1)$, we obtain

$$\tilde{f}_\varsigma(i) < \frac{1}{h^2 \Gamma(\varsigma + 1)} [-h^3 \varsigma(\varsigma - 1)(\varsigma - 2)] [x_i^{\varsigma-3} + (1-x_i)^{\varsigma-3}] \leq \frac{h(2-\varsigma)}{\Gamma(\varsigma - 1)} 2^{4-\varsigma} < 0. \quad (14)$$

which completes the proof of (13).

Another step is that A_h^β is an M-matrix. If $\beta \geq \beta_0$, then $a_{j,j+1}^{\beta,h} = a_{j+1,j}^{\beta,h} \leq 0$ for $j = 1, \dots, M-2$. The converse implication is also true. On this basis, the problem reduces to prove that $(A_h^\beta)^{-1}$ is nonnegative, which can be done easily by contradiction, see reference [39] for a proof.

120 It remains to prove (11). As the proof of the property 3, for the case when $h \leq 1/7$, by simple algebraic manipulations, we deduce

$$-\varsigma(\varsigma-1)(\varsigma-2)h^3 \left\{ 1 - \frac{1}{8}(\varsigma-3)h[(1-\xi_1)^{\varsigma-4} - 16(1-\xi_2)^{\varsigma-4} + 27(1-\xi_3)^{\varsigma-4}] \right\} < 0,$$

which leads to $\hat{f}_\varsigma(i) < (4-2^\varsigma)h^{\varsigma-2}/\Gamma(\varsigma+1)$ for $i = 1$ and $i = M-1$. Furthermore, together with (14), (11) is proved immediately. ■

For the purpose to ensure that $\mathcal{A}_{h\tau}^n$ is an M-matrix, below are two classes of sufficient conditions.

125 **Class 1.** $\beta \geq \beta_0$ and

$$\frac{\tau_n^{\alpha_0}}{h^{2\gamma}} > -\frac{4 \cos(\gamma\pi)\Gamma(4-2\gamma)}{3K_2(3^{3-2\gamma} - 2^{5-2\gamma} + 7)} \sum_{i=0}^s \frac{a_i}{\Gamma(3-\alpha_i)}. \quad (15)$$

Class 2. $\beta < \beta_0$ with a suitably small h satisfying

$$h^{2(\gamma-\beta)} < -\frac{1}{2} \frac{K_2(3^{3-2\gamma} - 2^{5-2\gamma} + 7)}{\cos(\gamma\pi)\Gamma(4-2\gamma)} \frac{\cos(\beta\pi)\Gamma(4-2\beta)}{K_1(3^{3-2\beta} - 2^{5-2\beta} + 7)} \quad (16)$$

and (15) concerning a given τ_n .

The upcoming theorem is singled out as an immediate consequence of Lemma 5 and Theorem 1.

Theorem 2. *The following properties are true for the coefficient matrix $\mathcal{A}_{h\tau}^n = (a_{i,j}^{h\tau})_{(M-1) \times (M-1)}$.*

- 130
1. $a_{i,i}^{h\tau} > 0$ for $i = 1, \dots, M-1$;
 2. $a_{i,j}^{h\tau} < 0$ for $|i-j| > 1$, $i, j = 1, \dots, M-1$;
 3. *It is strictly diagonally dominant.*

In addition, under either Class 1 or Class 2 of sufficient conditions, $\mathcal{A}_{h\tau}^n$ is further an M-matrix.

Proof. Properties 1, 2 and 3 are obvious facts by (7), (8), Lemma 5 and Theorem 1. Evidently, as 135 the proof in Theorem 1, if we can prove that the minor diagonal elements of $\mathcal{A}_{h\tau}^n$ are all negative under either class of sufficient conditions, then the M-matrix property of $\mathcal{A}_{h\tau}^n$ is established immediately.

In fact, the condition (15) is imposed to make

$$\sum_{i=0}^s \frac{a_i \tau_n^{-\alpha_i}}{3\Gamma(3-\alpha_i)} + \frac{1}{2} \frac{K_2(3^{3-2\gamma} - 2^{5-2\gamma} + 7)h^{-2\gamma}}{2 \cos(\gamma\pi)\Gamma(4-2\gamma)} < 0$$

valid, which further gives, due to $\tau_n^{\alpha_0 - \alpha_i} < 1$ ($\alpha_i < \alpha_0$, $i = 1, \dots, s$),

$$\sum_{i=0}^s \frac{a_i \tau_n^{-\alpha_i}}{3\Gamma(3 - \alpha_i)} + \frac{1}{2} \frac{K_2(3^{3-2\gamma} - 2^{5-2\gamma} + 7)h^{-2\gamma}}{2 \cos(\gamma\pi)\Gamma(4 - 2\gamma)} < 0. \quad (17)$$

For the case $\beta \geq \beta_0$, by Theorem 1 and (17), we can conclude that

$$\sum_{i=0}^s \frac{a_i \tau_n^{-\alpha_i}}{\Gamma(3 - \alpha_i)} \frac{h}{3} + \frac{K_1(3^{3-2\beta} - 2^{5-2\beta} + 7)h^{1-2\beta}}{2 \cos(\beta\pi)\Gamma(4 - 2\beta)} + \frac{K_2(3^{3-2\gamma} - 2^{5-2\gamma} + 7)h^{1-2\gamma}}{2 \cos(\gamma\pi)\Gamma(4 - 2\gamma)} < 0. \quad (18)$$

140 For the opposite $\beta < \beta_0$, we have $(3^{3-2\beta} - 2^{5-2\beta} + 7)/[2 \cos(\beta\pi)\Gamma(4 - 2\beta)] > 0$. Observe that the order gap $\gamma - \beta > 0$, there always exists a small h subject to (16). Apparently, this situation also yields (18). Furthermore, (18) implies, upon multiplying through the factor $\Gamma(3 - \alpha_0)\tau_n^{\alpha_0}/2$, that the minor diagonal elements of $\mathcal{A}_{h\tau}^n$ are all negative. Hence, results of Theorem 2 are obtained. ■

3. Condition number estimation and an adaptive AMG

145 This section is devoted to the derivation of the condition number estimation on $\mathcal{A}_{h\tau}^n$ and the proposal of an appropriate solver.

3.1. Condition number estimation

Theorem 3. For the matrix $\mathcal{A}_{h\tau}^n$ defined by (7), we have

$$\kappa(\mathcal{A}_{h\tau}^n) \lesssim 1 + \tau_n^{\alpha_0} h^{-2\gamma}. \quad (19)$$

Proof. Obviously, there is a spectral equivalence

$$\kappa(\mathcal{A}_{h\tau}^n) \simeq \kappa\left(\sum_{i=0}^s C_i \tau_n^{\alpha_0 - \alpha_i} I + \tilde{C}_1 \tau_n^{\alpha_0} M_h^{-\frac{1}{2}} A_h^\beta M_h^{-\frac{1}{2}} + \tilde{C}_2 \tau_n^{\alpha_0} M_h^{-\frac{1}{2}} A_h^\gamma M_h^{-\frac{1}{2}}\right), \quad (20)$$

150 where $C_i = a_i \Gamma(3 - \alpha_0)/\Gamma(3 - \alpha_i)$ and $\tilde{C}_j = K_j \Gamma(3 - \alpha_0)/2$ ($j = 1, 2$).

It is worthwhile to point out that the expressions

$$\lambda_{\min}(M_h^{-\frac{1}{2}} A_h^\gamma M_h^{-\frac{1}{2}}) \gtrsim 1, \quad \lambda_{\max}(M_h^{-\frac{1}{2}} A_h^\gamma M_h^{-\frac{1}{2}}) \lesssim h^{-2\gamma} \quad (21)$$

have been obtained by us based on Lemma 2, 3 and 5, as well as the Cauchy-Schwarz inequality [38]. Similarly, according to Lemma 2 and 3, we get

$$(A_h^\beta \vec{u}_h, \vec{u}_h) = \frac{1}{\cos(\beta\pi)} ({}_x D_L^\beta u_h, {}_x D_R^\beta u_h)_{L^2(\Omega)} \gtrsim (u_h, u_h)_{L^2(\Omega)} = (M_h \vec{u}_h, \vec{u}_h) \simeq h(\vec{u}_h, \vec{u}_h)$$

with $u_h := (\phi_1, \dots, \phi_{M-1})\vec{u}_h$ for an arbitrary vector $\vec{u}_h := (u_1^h, \dots, u_{M-1}^h)^T \in \mathbb{R}^{M-1}$. Moreover,
 155 on account of Theorem 1, we arrive at, for $\beta_0 \leq \beta < 1/2$,

$$(A_h^\beta \vec{u}_h, \vec{u}_h) \leq \sum_{i=1}^{M-1} a_{i,i}^{\beta,h} (u_i^h)^2 - \sum_{i=1}^{M-1} \sum_{j \neq i} a_{i,j}^{\beta,h} \frac{(u_i^h)^2 + (u_j^h)^2}{2} \leq 2a_{1,1}^{\beta,h} (\vec{u}_h, \vec{u}_h),$$

and, for $0 < \beta < \beta_0$,

$$\begin{aligned} (A_h^\beta \vec{u}_h, \vec{u}_h) &\leq \sum_{i=1}^{M-1} a_{i,i}^{\beta,h} (u_i^h)^2 + \sum_{i=1}^{M-1} \sum_{|j-i|=1} a_{i,j}^{\beta,h} \frac{(u_i^h)^2 + (u_j^h)^2}{2} - \sum_{i=1}^{M-1} \sum_{|j-i|>1} a_{i,j}^{\beta,h} \frac{(u_i^h)^2 + (u_j^h)^2}{2} \\ &= \sum_{i=1}^{M-1} (u_i^h)^2 \left[a_{i,i}^{\beta,h} + a_{i,i+1}^{\beta,h} + a_{i,i-1}^{\beta,h} - \sum_{j=i+2}^{M-1} a_{i,j}^{\beta,h} - \sum_{j=1}^{i-2} a_{i,j}^{\beta,h} \right] \leq 2(a_{1,1}^{\beta,h} + 2a_{1,2}^{\beta,h}) (\vec{u}_h, \vec{u}_h), \end{aligned}$$

which both indicate that $(A_h^\beta \vec{u}_h, \vec{u}_h) \lesssim h^{1-2\beta} (\vec{u}_h, \vec{u}_h)$, regardless of what sort of relationship between β and β_0 . Taking $\vec{v}_h = M_h^{\frac{1}{2}} \vec{u}_h$, yields

$$(\vec{v}_h, \vec{v}_h) \lesssim (M_h^{-\frac{1}{2}} A_h^\beta M_h^{-\frac{1}{2}} \vec{v}_h, \vec{v}_h) \lesssim h^{-2\beta} (\vec{v}_h, \vec{v}_h).$$

As the vector \vec{v}_h is arbitrary, the above expression can be rewritten as

$$\lambda_{\min}(M_h^{-\frac{1}{2}} A_h^\beta M_h^{-\frac{1}{2}}) \gtrsim 1, \quad \lambda_{\max}(M_h^{-\frac{1}{2}} A_h^\beta M_h^{-\frac{1}{2}}) \lesssim h^{-2\beta}. \quad (22)$$

160 Combining (20), (21), (22) and noting that $C_0 = a_0 > 0$, $K_1 > 0$ and $K_2 > 0$, give rise to

$$\kappa(\mathcal{A}_{h\tau}^n) \lesssim \frac{\sum_{i=0}^s C_i \tau_n^{\alpha_0 - \alpha_i} + \tilde{C}_1 \tau_n^{\alpha_0} h^{-2\beta} + \tilde{C}_2 \tau_n^{\alpha_0} h^{-2\gamma}}{\sum_{i=0}^s C_i \tau_n^{\alpha_0 - \alpha_i} + \tilde{C}_1 \tau_n^{\alpha_0} + \tilde{C}_2 \tau_n^{\alpha_0}} \lesssim 1 + \tau_n^{\alpha_0} h^{-2\gamma},$$

which completes the proof. ■

Remark 3. *The relation (19) is obviously a generalization of the estimation on resulting matrices from traditional parabolic differential equations, single-term time FDEs and FADEs.*

An immediate corollary of the above theorem follows with great practical interest.

165 **Corollary 1.** *Let the current time step size $\tau_n = \mathcal{O}(h^\varrho)$ and satisfy $\varrho\alpha_0 \geq 2\gamma$. Then we have*

$$\kappa(\mathcal{A}_{h\tau}^n) = \mathcal{O}(1). \quad (23)$$

3.2. Classical AMG with convergence analysis and its adaptive variant

Nowadays, classical AMG is quite mature and capable of various ill-conditioned Toeplitz systems. Most of the existing AMG software packages (e.g. FASP [40], BoomerAMG [41] and AmgX [42])

are built on it. It has Setup and Solve phases. The former phase builds all the ingredients required
 170 by a hierarchy of grids, the finest to the coarsest, while the latter phase runs V-cycle, W-cycle or
 F-cycle until the desired convergence is achieved, where the smoother and the coarse-grid correction
 are crucial components. It should be emphasized that damped-Jacobi becomes a favorable smoother
 for the system (6), since it can be executed by FFT to retain the $\mathcal{O}(M \log M)$ complexity.

Next we turn to the theoretical analysis when $\mathcal{A}_{h\tau}^n$ is a strictly diagonally dominant M-matrix. We
 175 here only assess two-level V(0,1)-cycle, viz., 0 pre-smoothing but 1 post-smoothing step is performed
 per V-cycle. It is advantageous to reorder the system (6) and the coarse-to-fine interpolation \mathcal{P} in
 reference to a given C/F splitting

$$\mathcal{A}_{h\tau}^n \mathcal{U}_{h\tau}^n = \begin{pmatrix} \mathcal{A}_{FF} & \mathcal{A}_{FC} \\ \mathcal{A}_{CF} & \mathcal{A}_{CC} \end{pmatrix} \begin{pmatrix} \mathcal{U}_F \\ \mathcal{U}_C \end{pmatrix} = \begin{pmatrix} \mathcal{F}_F \\ \mathcal{F}_C \end{pmatrix} = \mathcal{F}_{h\tau}^n, \quad \mathcal{P} = \begin{pmatrix} \mathcal{P}_{FC} \\ \mathcal{I}_{CC} \end{pmatrix}$$

with \mathcal{I}_{CC} as the identity. Another basic tools are specific norms of any vector $v = (v_F, v_C)^T \in \mathbb{R}^{M-1}$

$$\|v_F\|_{0,F} = (\text{diag}(\mathcal{A}_{FF})v_F, v_F)^{\frac{1}{2}}, \quad \|v\|_1 = (\mathcal{A}_{h\tau}^n v, v)^{\frac{1}{2}}, \quad \|v\|_2 = (\text{diag}^{-1}(\mathcal{A}_{h\tau}^n)\mathcal{A}_{h\tau}^n v, \mathcal{A}_{h\tau}^n v)^{\frac{1}{2}}.$$

It can easily be derived that the two-level iteration matrix to be considered is

$$\mathcal{M}_{h,H} = \mathcal{S}_h [\mathcal{I} - \mathcal{P}(\mathcal{P}^T \mathcal{A}_{h\tau}^n \mathcal{P})^{-1} \mathcal{P}^T \mathcal{A}_{h\tau}^n],$$

180 where \mathcal{S}_h is the post-smoothing iteration matrix. Using the two-level convergence theory in [28] and
 Theorem 2, the following theorem states an uniform upper bound for $\mathcal{M}_{h,H}$.

Theorem 4. *Let \mathcal{S}_h be damped-Jacobi or Gauss-Seidel relaxation and \mathcal{P} be the direct interpolation. For a given C/F splitting, under either Class 1 or Class 2 of sufficient conditions, there exist constants $\sigma_2 \geq 1 > \sigma_1 > 0$ independent of step sizes τ_n and h , such that*

$$\|\mathcal{M}_{h,H}\|_1 \leq \sqrt{1 - \frac{\sigma_1}{\sigma_2}}. \quad (24)$$

185 **Proof.** By Theorem A.4.1 and A.4.2 in [28], (24) is valid if we provide that \mathcal{S}_h satisfies the smoothing
 property

$$\|\mathcal{S}_h e_h\|_1^2 \leq \|e_h\|_1^2 - \sigma_1 \|e_h\|_2^2 \quad (25)$$

and \mathcal{P} meets the accuracy property

$$\|e_F - \mathcal{P}_{FC} e_C\|_{0,F}^2 \leq \sigma_2 \|e_h\|_1^2 \quad (26)$$

for all $e_h = (e_F^T, e_C^T)^T \in \mathbb{R}^{M-1}$.

We start with (25). According to Theorem A.3.1 and A.3.2 in [28], it is valid for damped-Jacobi relaxation (parameter $0 < \omega < 2/\eta$) with $\sigma_1 = \omega(2 - \omega\eta)$, and for Gauss-Seidel relaxation with $\sigma_1 = 1/[(1 + \gamma_-)(1 + \gamma_+)]$, where

$$\eta \geq \rho(\text{diag}^{-1}(\mathcal{A}_{h\tau}^n)\mathcal{A}_{h\tau}^n), \quad \gamma_- = \max_i \left\{ \frac{1}{w_i a_{i,i}^{h\tau}} \sum_{j < i} w_j |a_{i,j}^{h\tau}| \right\}, \quad \gamma_+ = \max_i \left\{ \frac{1}{w_i a_{i,i}^{h\tau}} \sum_{j > i} w_j |a_{i,j}^{h\tau}| \right\},$$

$\vec{w} = (w_1, \dots, w_{M-1})^T$ is an arbitrary vector with \vec{w} and $\mathcal{A}_{h\tau}^n \vec{w}$ both being positive. Recall Theorem 2, one immediately obtains $0 < \gamma_- < 1$, $0 < \gamma_+ < 1$ and

$$\rho(\text{diag}^{-1}(\mathcal{A}_{h\tau}^n)\mathcal{A}_{h\tau}^n) \leq |\text{diag}^{-1}(\mathcal{A}_{h\tau}^n)\mathcal{A}_{h\tau}^n|_{\vec{w}} = \max_i \left\{ \frac{1}{w_i} \sum_j w_j \frac{|a_{i,j}^{h\tau}|}{a_{i,i}^{h\tau}} \right\} < 2.$$

These indicate $\sigma_1 \leq 1/\eta < 1$ for damped-Jacobi and $\sigma_1 \in (1/4, 1)$ for Gauss-Seidel, both independent of e_h , τ_n and h . It is worth noting that Jacobi relaxation is always available, since there exists a small distance ϵ so that $\eta = 2 - \epsilon \geq \rho(\text{diag}^{-1}(\mathcal{A}_{h\tau}^n)\mathcal{A}_{h\tau}^n)$.

It remains to prove the second part (26). Through Theorem A.4.3 in [28], \mathcal{P}_{FC} holds (26) with

$$\sigma_2 \geq \max_{i \in F} \left\{ \frac{\sum_{j \in N_i} a_{i,j}^{h\tau}}{\sum_{j \in P_i} a_{i,j}^{h\tau}} \right\},$$

where the neighborhood $N_i = \{j \neq i : a_{i,j}^{h\tau} \neq 0\}$, P_i is the set of interpolatory variables at F-point i . Notice the fact that Ruge-Stüben coarsening strategy retains $i-1 \in P_i$ or $i+1 \in P_i$ using properties of $\mathcal{A}_{h\tau}^n$. It implies that $\sigma_2 \geq 1$ independent of e_h due to $a_{i,j}^{h\tau} < 0$ for $j \in N_i$ from Theorem 2, and

$$\frac{\sum_{j \in N_i} a_{i,j}^{h\tau}}{\sum_{j \in P_i} a_{i,j}^{h\tau}} < -\frac{a_{i,i}^{h\tau}}{a_{i,i-1}^{h\tau}} = -\frac{a_{i,i}^{h\tau}}{a_{i,i+1}^{h\tau}} = -\frac{4C_1 + 3C_2\tau_n^{\alpha_0}h^{-2\gamma}}{C_1 + 3C_3\tau_n^{\alpha_0}h^{-2\gamma}}, \quad (27)$$

where

$$C_1 = \sum_{i=0}^s a_i \frac{\tau_n^{\alpha_0 - \alpha_i}}{\Gamma(3 - \alpha_i)}, \quad C_2 = K_1 \frac{h^{2(\gamma-\beta)}(2^{4-2\beta} - 8)}{2 \cos(\beta\pi)\Gamma(4 - 2\beta)} + K_2 \frac{2^{4-2\gamma} - 8}{2 \cos(\gamma\pi)\Gamma(4 - 2\gamma)}$$

and

$$C_3 = K_1 \frac{h^{2(\gamma-\beta)}(3^{3-2\beta} - 2^{5-2\beta} + 7)}{2 \cos(\beta\pi)\Gamma(4 - 2\beta)} + K_2 \frac{3^{3-2\gamma} - 2^{5-2\gamma} + 7}{2 \cos(\gamma\pi)\Gamma(4 - 2\gamma)}.$$

Plugging (15), along with (16) when $\beta < \beta_0$, (31) suggests that σ_2 isn't tied to τ_n and h . Therefore (24) is proved. ■

Remark 4. The upper bound (24) tells us that a much faster convergence of the two-level $V(0,1)$ -cycle will be achieved if σ_1/σ_2 can be made quite closer to 1.

Table 1 is offered in support of Theorem 4. It is easy to see that the uniform convergence of the two-level V(0,1)-cycle is achieved. Nevertheless, the strength-of-connection tolerance θ , used to interpret concepts of strong influence and dependence, has a significantly negative impact on its actual number of iterations.

Table 1: Effect of θ on the two-level V(0,1)-cycle with 10^{-8} as the tolerance for stopping.

M	$\alpha_0 = 0.9, \alpha_1 = 0.4, \beta = 0.3, \gamma = 0.8$			$\alpha_0 = 0.7, \alpha_1 = 0.5, \beta = 0.15, \gamma = 0.95$		
	$\theta = 0.0001$	$\theta = 0.005$	$\theta = 0.25$	$\theta = 0.0001$	$\theta = 0.005$	$\theta = 0.25$
512	292	36	13	191	35	15
1024	308	38	13	198	35	15
2048	314	36	13	202	35	15

It is well to be reminded that multigrid V(1,1)-cycle in CF-relaxation is of a larger practical value in applications. In this situation, the impact becomes rather serious. Table 2 shows the results of $\alpha_0 = 0.7, \alpha_1 = 0.5, \beta = 0.15, \gamma = 0.95$.

Table 2: Effect of θ on multigrid V(1,1)-cycle in CF-relaxation with 10^{-12} as the tolerance for stopping.

M	$\theta = 0.0001$			$\theta = 0.03529$			$\theta = 0.03533$		
	Levels	Iterations	CPU	Levels	Iterations	CPU	Levels	Iterations	CPU
512	3	224	6.08E-1	6	21	1.38E-1	7	5	3.80E-2
1024	3	226	2.53E0	7	23	5.42E-1	8	5	1.55E-1
2048	4	227	1.02E1	8	25	2.23E0	9	5	6.17E-1

As indicated, there are two drawbacks to multigrid V(1,1)-cycle in CF-relaxation. One lies the good choice of θ . We have discussed the most reliable $\theta = a_{1,3}^{h\tau}/a_{1,2}^{h\tau} + \epsilon_0$ for time-space Caputo-Riesz FDEs [38], where ϵ_0 is some small number. However, it may cause the method lack of convergence optimality because of positive minor diagonal elements of A_h^β when $\beta < \beta_0$, e.g. in Table 2, $a_{1,3}^{h\tau}/a_{1,2}^{h\tau} \approx 0.035285$ for the case $M = 512$, but 0.03529 isn't the optimal value of θ . A natural cure technique for this is to employ

$$\theta^{(k)} = \frac{a_{1,3}^{(k)}}{a_{1,2}^{(k)}} + \epsilon_0 \quad (28)$$

for the k -th coarse-level Galerkin matrix $\mathcal{A}_k = (a_{i,j}^{(k)})$ with $\mathcal{A}_0 = \mathcal{A}_{h\tau}^n$. Indeed, $\max_k(\theta^{(k)}) \approx 0.03533$ to obtain the optimal convergence. The other is the required cost of $\mathcal{O}(M^2)$ at each time step. This drawback hampers the acceptance of the method in large linear systems. The primary reason is that

it is impossible to make $\mathcal{A}_1 = \mathcal{P}^T \mathcal{A}_0 \mathcal{P}$ Toeplitz-like by direct interpolation in a straightforward way. This requests for a modification to \mathcal{P} . The following lemma provides a proper manipulation.

225 **Lemma 6.** *If \mathcal{P}_{FC} admits 1/2 as all nonzero entries based on the choice (28), then \mathcal{A}_1 must be a symmetric Toeplitz matrix.*

Proof. Obviously, $\mathcal{A}_1^T = (\mathcal{P}^T \mathcal{A}_0 \mathcal{P})^T = \mathcal{P}^T \mathcal{A}_0 \mathcal{P} = \mathcal{A}_1$, and

$$a_{i,i+l}^{(1)} = a_{i+l,i}^{(1)} = \frac{1}{4}a_{3,2l+1}^{h\tau} + a_{2,2l+1}^{h\tau} + \frac{3}{2}a_{1,2l+1}^{h\tau} + a_{1,2l+2}^{h\tau} + \frac{1}{4}a_{1,2l+3}^{h\tau}, \quad i = 1, \dots, M_1 - l,$$

where M_1 is the number of columns of \mathcal{P}_{FC} . This completes the proof. ■

230 **Remark 5.** *It can easily be seen that just $\mathcal{O}(M_1)$ operations are required to generate \mathcal{A}_1 (only M_1 different entries), whose cost is negligible relative to that of direct interpolation.*

More interestingly, the two-level convergence for the modified interpolation is also uniform as a result of the following theorem.

Theorem 5. *Let $h \leq 1/7$ and \mathcal{P}_{FC} satisfy Lemma 6. For a given C/F splitting, under either Class 1 or Class 2 of sufficient conditions, there exists a constant $\sigma_2 \geq 1$ independent of step sizes τ_n and h , such that the accuracy property (26) holds for all $e_h = (e_F^T, e_C^T)^T = (e_1, e_2, \dots, e_{M-1})^T \in \mathbb{R}^{M-1}$.*

Proof. To estimate the right part, we note

$$\|e_h\|_1^2 = (\mathcal{A}_{h\tau}^n e_h, e_h) \geq \sum_{i \in F} \left[\sum_{k \in P_i} (-a_{i,k}^{h\tau})(e_i - e_k)^2 + \sum_j a_{i,j}^{h\tau} e_i^2 \right]. \quad (29)$$

On the other hand, we can estimate

$$\|e_F - \mathcal{P}_{FC} e_C\|_{0,F}^2 = \sum_{i \in F} a_{i,i}^{h\tau} \left(e_i - \sum_{k \in P_i} \frac{1}{2} e_k \right)^2 \leq \sum_{i \in F} a_{i,i}^{h\tau} \sum_{k \in P_i} \frac{1}{2} (e_i - e_k)^2 + a_{1,1}^{h\tau} (e_1^2 + e_{M-1}^2), \quad (30)$$

employing Schwarz inequality and the fact that Ruge-Stüben coarsening strategy guarantees $i - 1$ or $i + 1$ inside of set P_i at F-point i . The previous estimations (29) and (30) imply (26), if relations 240 $\sigma_2(-a_{i,k}^{h\tau}) \geq a_{i,i}^{h\tau}/2$ as well as $\sigma_2 \sum_{j=1}^{M-1} a_{1,j}^{h\tau} \geq a_{1,1}^{h\tau}$ hold simultaneously for $k \in P_i$ and $i \in F$, namely

$$\sigma_2 \geq \max_{i \in F} \left\{ -\frac{a_{i,i}^{h\tau}}{2a_{i,i-1}^{h\tau}}, \frac{a_{1,1}^{h\tau}}{\sum_{j=1}^{M-1} a_{1,j}^{h\tau}} \right\}. \quad (31)$$

It indicates that $\sigma_2 \geq 1$ independent of e_h . Furthermore, observing (7), (8), (10) and (11), yield

$$\frac{a_{1,1}^{h\tau}}{\sum_{j=1}^{M-1} a_{1,j}^{h\tau}} < 2, \quad -\frac{a_{i,i}^{h\tau}}{2a_{i,i-1}^{h\tau}} = -\frac{4C_1 + 3(K_1 C_2^\beta h^{2(\gamma-\beta)} + K_2 C_2^\gamma) \tau_n^{\alpha_0} h^{-2\gamma}}{2C_1 + 6(K_1 C_3^\beta h^{2(\gamma-\beta)} + K_2 C_3^\gamma) \tau_n^{\alpha_0} h^{-2\gamma}},$$

where

$$C_1 = \sum_{i=0}^s a_i \frac{\tau_n^{\alpha_0 - \alpha_i}}{\Gamma(3 - \alpha_i)}, \quad C_2^e = \frac{2^{4-2e} - 8}{2 \cos(\varrho\pi)\Gamma(4 - 2\varrho)}, \quad C_3^e = \frac{3^{3-2e} - 2^{5-2e} + 7}{2 \cos(\varrho\pi)\Gamma(4 - 2\varrho)}.$$

Plugging (15), along with (16) when $\beta < \beta_0$, (31) suggests that σ_2 isn't tied to τ_n or h at all. This establishes the result. ■

245 It should be stressed that these previous procedures can be performed similarly with multigrid to render all \mathcal{A}_k ($k \geq 2$) Toeplitz-like. Two practical benefits involve computational cost of $\mathcal{O}(M \log M)$ and matrix-free storage of $\mathcal{O}(M)$. Additionally, it is easy to verify that \mathcal{A}_k ($k \geq 1$) could also be an M-matrix for small k constrained by (15) with h being replaced by $2^k h$, together with (16) if $\beta < \beta_0$.

We conclude this section by developing an adaptive AMG algorithm, which exploits features of 250 FFT, Toeplitz-like structures of \mathcal{A}_k ($k \geq 0$) and at most 2 nonzeros per row in interpolations, while Corollary 1 as our clear distinction.

Algorithm 1. *An adaptive AMG for the system (6).*

Step 1. *If $\mathcal{A}_{h\tau}^n$ satisfies the estimation (23), then solve (6) by conjugate gradient (CG) algorithm.*

Step 2. *Apply the improved classical AMG to solve (6) until convergence.*

255 **2.1 Setup phase.**

2.1.1 *Set $\epsilon_0 = 10^{-8}$, max_cdofs , max_levels , $j = 0$ and $\Omega^{(0)} = \{1, 2, \dots, M - 1\}$.*

2.1.2 *Compute $\theta^{(j)}$ via (28), perform $\Omega^{(j)} = C^{(j)} \cup F^{(j)}$, and set $\Omega^{(j+1)} = C^{(j)}$.*

2.1.3 *Construct the modified $\mathcal{P}^{(j)}$ and $\mathcal{A}_{j+1} = (\mathcal{P}^{(j)})^T \mathcal{A}_j \mathcal{P}^{(j)}$.*

2.1.4 *If $|\Omega^{(j+1)}| \leq \text{max_cdofs}$ or $j + 1 = \text{max_levels}$, then Stop; else $j = j + 1$, goto 2.1.2.*

260 **2.2 Solve phase: $V(1,1)$ -cycle.** *Set $\mathcal{F}_0 = \mathcal{F}_{h\tau}^n$ and choose an initial guess \mathcal{U}_0 .*

2.2.1 *For $k = 0, 1, \dots, j$, do:*

- *Run Jacobi relaxation once to $\mathcal{A}_k \mathcal{U}_k = \mathcal{F}_k$ with $\mathcal{U}_k = 0$ ($k > 0$).*
- *Compute $\mathcal{F}_{k+1} = (\mathcal{P}^{(k)})^T (\mathcal{F}_k - \mathcal{A}_k \mathcal{U}_k)$.*

2.2.2 *Solve $\mathcal{A}_{j+1} \mathcal{U}_{j+1} = \mathcal{F}_{j+1}$ by using Gaussian elimination without pivoting.*

265 **2.2.3** *For $k = j, j - 1, \dots, 0$, do:*

- *Update $\mathcal{U}_k = \mathcal{U}_k + \mathcal{P}^{(k)} \mathcal{U}_{k+1}$.*
- *Run Jacobi relaxation once to $\mathcal{A}_k \mathcal{U}_k = \mathcal{F}_k$.*

4. Numerical results

In this section we will present some numerical experiments to illustrate the convergence of our time-space FE numerical scheme (5), the correctness of our condition number estimation and the effectiveness of our solver. All examples are implemented in C on a 64 bit Fedora 18 platform with an -O2 optimization parameter, double precision arithmetic on Intel Xeon (W5590) with configurations 24.0 GB RAM and 3.33 GHz.

In our implementations, all integrals are calculated by a quadrature formula. In tables below, columns labeled $\|e\|_0$ represent errors $\|u(\cdot, T) - u_{h\tau}(\cdot, T)\|_{L^2(\Omega)}$, λ_{\min} denote the smallest eigenvalues and λ_{\max} as the largest eigenvalues, κ are condition numbers of resulting matrices, *Its* indicate numbers of iterations until the actual residual is reduced by a factor of 10^{-12} , T_c express CPU times including Setup and Solve phases with second as the unit, starred entries (*) indicate the solutions fail to converge after 1000 iterations, while CG, CAMG and *i*CAMG stand for conjugate gradient, classical AMG and the adaptive variant in Algorithm 1, respectively.

4.1. Convergence test

Example 1. Consider problem (1)-(3) with $s = 1$, $a_0 = a_1 = 1$, $K_1 = 1$, $K_2 = 2$, $T = 0.5$, $\Omega = (0, 1)$, $\psi_0(x) = 100(x^2 - x^3)$ and

$$f(x, t) = 200(x^2 - x^3) \left[\frac{t^{2-\alpha_0}}{\Gamma(3-\alpha_0)} + \frac{t^{2-\alpha_1}}{\Gamma(3-\alpha_1)} \right] + \frac{50(t^2+1)}{\cos(\beta\pi)} \times \left[\frac{(1-x)^{1-2\beta}}{\Gamma(2-2\beta)} + \frac{2x^{2-2\beta} - 4(1-x)^{2-2\beta}}{\Gamma(3-2\beta)} + \frac{6(1-x)^{3-2\beta} - 6x^{3-2\beta}}{\Gamma(4-2\beta)} \right] + \frac{100(t^2+1)}{\cos(\gamma\pi)} \times \left[\frac{(1-x)^{1-2\gamma}}{\Gamma(2-2\gamma)} + \frac{2x^{2-2\gamma} - 4(1-x)^{2-2\gamma}}{\Gamma(3-2\gamma)} + \frac{6(1-x)^{3-2\gamma} - 6x^{3-2\gamma}}{\Gamma(4-2\gamma)} \right].$$

The exact solution is $u(x, t) = 100(t^2 + 1)(x^2 - x^3)$. Table 3 and 4 show the results of errors and convergence rates with typical α_0 , α_1 , β and γ for two specific cases: $h = \tau$ and $h = \sqrt{\tau}$, respectively. An interpretation is that the time-space FE solution possesses the saturation error order $\mathcal{O}(\tau^2 + h^2)$. Fig. 1 illustrates the exact solution with the numerical solution of $\alpha_0 = 0.7$, $\alpha_1 = 0.4$, $\beta = 0.15$, $\gamma = 0.95$ when $h = \tau = 1/64$.

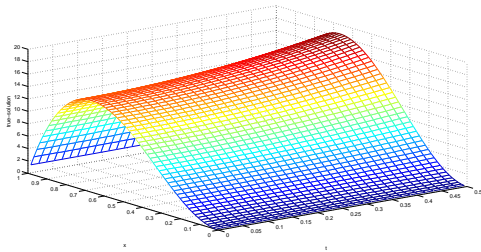
Example 2. Consider problem (1)-(3) with $s = 1$, $a_0 = a_1 = 1$, $T = 0.5$, $\Omega = (0, 1)$, $\psi_0(x) =$

Table 3: Error results and convergence rates in spatial direction with $h = \tau$.

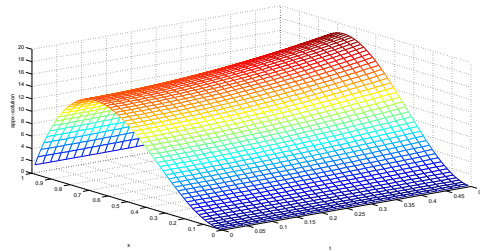
M	$\alpha_0 = 0.5, \alpha_1 = 0.2$				$\alpha_0 = 0.7, \alpha_1 = 0.4$			
	$\beta = 0.3, \gamma = 0.8$		$\beta = 0.15, \gamma = 0.95$		$\beta = 0.3, \gamma = 0.8$		$\beta = 0.15, \gamma = 0.95$	
	$\ e\ _0$	rate	$\ e\ _0$	rate	$\ e\ _0$	rate	$\ e\ _0$	rate
16	6.837E-2	-	8.357E-2	-	6.396E-2	-	8.186E-2	-
32	1.525E-2	2.165	2.020E-2	2.049	1.458E-2	2.133	1.981E-2	2.047
64	3.484E-3	2.130	4.878E-3	2.050	3.383E-3	2.108	4.811E-3	2.042
128	8.113E-4	2.102	1.183E-3	2.044	7.948E-4	2.089	1.171E-3	2.039

Table 4: Error results and convergence rates in spatial direction with $h = \sqrt{\tau}$.

N	$\alpha_0 = 0.5, \alpha_1 = 0.2$				$\alpha_0 = 0.7, \alpha_1 = 0.4$			
	$\beta = 0.3, \gamma = 0.8$		$\beta = 0.15, \gamma = 0.95$		$\beta = 0.3, \gamma = 0.8$		$\beta = 0.15, \gamma = 0.95$	
	$\ e\ _0$	rate	$\ e\ _0$	rate	$\ e\ _0$	rate	$\ e\ _0$	rate
32	2.600E-1	-	3.182E-1	-	2.582E-1	-	3.164E-1	-
128	5.929E-2	1.066	7.719E-2	1.022	5.899E-2	1.065	7.692E-2	1.020
512	1.369E-2	1.057	1.877E-2	1.020	1.362E-2	1.058	1.871E-2	1.020
2048	3.194E-3	1.050	4.569E-3	1.019	3.177E-3	1.050	4.554E-3	1.019



(a) The exact solution



(b) The numerical solution

Figure 1: Comparison on solutions, $h = \tau = 1/64$, $\alpha_0 = 0.7$, $\alpha_1 = 0.4$, $\beta = 0.15$, $\gamma = 0.95$.

$100x^2(1-x)^2$ and

$$f(x, t) = 200x^2(1-x)^2 \left[\frac{t^{2-\alpha_0}}{\Gamma(3-\alpha_0)} + \frac{t^{2-\alpha_1}}{\Gamma(3-\alpha_1)} \right] + \frac{100K_1(t^2+1)}{\cos(\beta\pi)} \times \left[\frac{x^{2-2\beta} + (1-x)^{2-2\beta}}{\Gamma(3-2\beta)} - \frac{6x^{3-2\beta} + 6(1-x)^{3-2\beta}}{\Gamma(4-2\beta)} + \frac{12x^{4-2\beta} + 12(1-x)^{4-2\beta}}{\Gamma(5-2\beta)} \right] + \frac{100K_2(t^2+1)}{\cos(\gamma\pi)} \times \left[\frac{x^{2-2\gamma} + (1-x)^{2-2\gamma}}{\Gamma(3-2\gamma)} - \frac{6x^{3-2\gamma} + 6(1-x)^{3-2\gamma}}{\Gamma(4-2\gamma)} + \frac{12x^{4-2\gamma} + 12(1-x)^{4-2\gamma}}{\Gamma(5-2\gamma)} \right].$$

The exact solution is $u(x, t) = 100(t^2+1)x^2(1-x)^2$. The objective of this example is to measure the possible effects of K_1 and K_2 on the convergence. Setting $K_1 = 5$ and $K_2 = 30, 300, 10^3$ and 10^6 , we can observe from Table 5 and 6 that time-space FE solutions retain $\mathcal{O}(\tau^2 + h^2)$, without any ties to K_1 nor K_2 . Fig. 2 charts the exact and numerical solutions distributed over $[0, 1] \times [0, 0.5]$ when $K_1 = 5, K_2 = 30$. This comparison demonstrates that the time-space FE solution confirms the exact solution very well.

Table 5: Error results and convergence rates in spatial direction with $\alpha_0 = 0.7, \alpha_1 = 0.4, \beta = 0.3, \gamma = 0.85$.

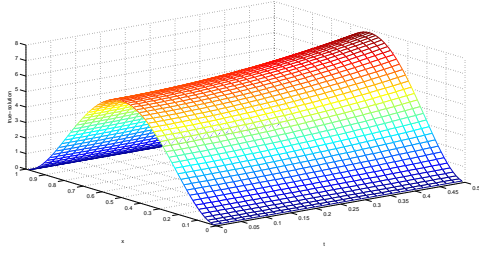
M	$h = \tau$				N	$h = \sqrt{\tau}$			
	$K_1 = 5, K_2 = 30$		$K_1 = 5, K_2 = 300$			$K_1 = 5, K_2 = 30$		$K_1 = 5, K_2 = 300$	
	$\ e\ _0$	rate	$\ e\ _0$	rate		$\ e\ _0$	rate	$\ e\ _0$	rate
16	3.455E-2	-	3.607E-2	-	32	1.305E-1	-	1.368E-1	-
32	8.466E-3	2.029	8.774E-3	2.040	128	3.065E-2	1.045	3.302E-2	1.026
64	1.987E-3	2.090	2.121E-3	2.049	512	7.362E-3	1.029	7.509E-3	1.068
128	4.509E-4	2.140	5.228E-4	2.020	2048	1.774E-3	1.027	1.792E-3	1.034

Table 6: Error results and convergence rates in spatial direction with $\alpha_0 = 0.8, \alpha_1 = 0.3, \beta = 0.2, \gamma = 0.75$.

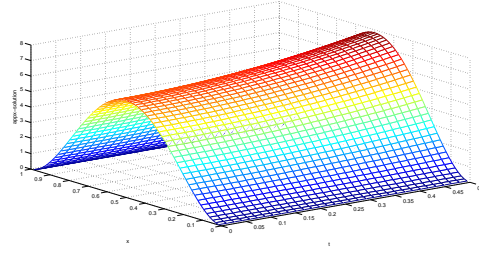
M	$h = \tau$				N	$h = \sqrt{\tau}$			
	$K_1 = 5, K_2 = 10^3$		$K_1 = 5, K_2 = 10^6$			$K_1 = 5, K_2 = 10^3$		$K_1 = 5, K_2 = 10^6$	
	$\ e\ _0$	rate	$\ e\ _0$	rate		$\ e\ _0$	rate	$\ e\ _0$	rate
16	3.544E-2	-	3.571E-2	-	32	1.350E-01	-	1.418E-01	-
32	8.635E-3	2.037	8.844E-3	2.013	128	3.221E-02	1.034	3.567E-02	0.996
64	2.065E-3	2.064	2.187E-3	2.016	512	6.905E-03	1.111	8.720E-03	1.016
128	4.916E-4	2.071	5.415E-4	2.014	2048	1.589E-03	1.060	2.047E-03	1.045

4.2. Condition number test

Example 3. We use the same Example 1.



(a) The exact solution



(b) The numerical solution

Figure 2: Comparison on solutions, $h = \tau = 1/64$, $K_1 = 5$, $K_2 = 30$, $\alpha_0 = 0.7$, $\alpha_1 = 0.4$, $\beta = 0.3$, $\gamma = 0.85$.

295

In this test, we examine the effectiveness of our estimation (19) in three situations: $\tau = h$, $\tau = h^2$ and $\tau = 1/64$. Results are summarized in Table 7, 8 and 9. We observe that they all coincide uniformly with Theorem 3.

Table 7: The smallest and largest eigenvalues, condition numbers and ratios with $\tau = h$.

M	$\alpha_0 = 0.9, \alpha_1 = 0.4, \beta = 0.3, \gamma = 0.8$				$\alpha_0 = 0.7, \alpha_1 = 0.5, \beta = 0.15, \gamma = 0.95$			
	λ_{\min}	λ_{\max}	κ	$ratio$	λ_{\min}	λ_{\max}	κ	$ratio$
64	1.938E-2	6.982E-1	3.603E+1	-	3.049E-2	9.275E+0	3.042E+2	-
128	8.941E-3	5.648E-1	6.316E+1	0.570	1.315E-2	1.065E+1	8.101E+2	0.376
256	4.252E-3	4.576E-1	1.076E+2	0.587	5.881E-3	1.224E+1	2.081E+3	0.389
512	2.061E-3	3.712E-1	1.801E+2	0.598	2.705E-3	1.405E+1	5.196E+3	0.400

Table 8: The smallest and largest eigenvalues, condition numbers and ratios with $\tau = h^2$.

M	$\alpha_0 = 0.9, \alpha_1 = 0.4, \beta = 0.3, \gamma = 0.8$				$\alpha_0 = 0.7, \alpha_1 = 0.5, \beta = 0.15, \gamma = 0.95$			
	λ_{\min}	λ_{\max}	κ	$ratio$	λ_{\min}	λ_{\max}	κ	$ratio$
32	3.230E-2	4.853E-2	1.503E+0	-	4.060E-2	7.249E-1	1.785E+1	-
64	1.585E-2	2.191E-2	1.382E+0	1.087	1.870E-2	5.103E-1	2.729E+1	0.654
128	7.864E-3	1.003E-2	1.275E+0	1.084	8.888E-3	3.596E-1	4.046E+1	0.674
256	3.918E-3	4.662E-3	1.190E+0	1.072	4.297E-3	2.537E-1	5.904E+1	0.685

Example 4. We use the same Example 2.

This example reveals the effect of K_2 on condition numbers of typical cases $\tau = h$, $\tau = h^2$ and $\tau = 1/64$ for $\alpha_0 = 0.7$, $\alpha_1 = 0.4$, $\beta = 0.3$, $\gamma = 0.85$ and $\alpha_0 = 0.8$, $\alpha_1 = 0.3$, $\beta = 0.2$, $\gamma = 0.75$. As

300

Table 9: The smallest and largest eigenvalues, condition numbers and ratios with $\tau = 1/64$.

M	$\alpha_0 = 0.9, \alpha_1 = 0.4, \beta = 0.3, \gamma = 0.8$				$\alpha_0 = 0.7, \alpha_1 = 0.5, \beta = 0.15, \gamma = 0.95$			
	λ_{\min}	λ_{\max}	κ	$ratio$	λ_{\min}	λ_{\max}	κ	$ratio$
64	1.938E-2	6.982E-1	3.603E+1	-	3.049E-2	9.275E+0	3.042E+2	-
128	9.691E-3	1.052E+0	1.085E+2	0.332	1.525E-2	1.730E+1	1.135E+3	0.268
256	4.846E-3	1.590E+0	3.281E+2	0.331	7.625E-3	3.229E+1	4.234E+3	0.268
512	2.423E-3	2.408E+0	9.939E+2	0.330	3.813E-3	6.025E+1	1.580E+4	0.268

expected, the results shown in Table 10 declare that condition numbers are independent of K_2 when K_2 is large enough.

Table 10: The condition numbers and ratios for Example 4.

K_2	$\alpha_0 = 0.7, \alpha_1 = 0.4, \beta = 0.3, \gamma = 0.85$						$\alpha_0 = 0.8, \alpha_1 = 0.3, \beta = 0.2, \gamma = 0.75$					
	$h = \tau$		$h = \sqrt{\tau}$		$\tau = 1/64$		$h = \tau$		$h = \sqrt{\tau}$		$\tau = 1/64$	
	κ	$ratio$	κ	$ratio$	κ	$ratio$	κ	$ratio$	κ	$ratio$	κ	$ratio$
3E2	5.06E3	-	3.77E2	-	5.21E3	-	1.63E3	-	1.12E2	-	1.75E3	-
3E3	5.31E3	0.95	4.89E2	0.77	5.33E3	0.98	1.81E3	0.90	2.07E2	0.54	1.82E3	0.96
3E4	5.34E3	0.99	5.04E2	0.97	5.34E3	0.99	1.83E3	0.99	2.26E2	0.91	1.83E3	0.99
3E5	5.34E3	1.00	5.06E2	1.00	5.34E3	1.00	1.83E3	1.00	2.28E2	0.99	1.83E3	1.00

4.3. Performance evaluation test

Example 5. Comparisons of *i*CAMG over CG and CAMG with Ruge-Stüben coarsening strategy

and $\mathcal{U}_0 = 0$.

Table 11: Number of iterations and wall time for the case $\tau = h$.

M	$\alpha_0 = 0.9, \alpha_1 = 0.4, \beta = 0.3, \gamma = 0.8$						$\alpha_0 = 0.7, \alpha_1 = 0.5, \beta = 0.15, \gamma = 0.95$					
	CG		CAMG		<i>i</i> CAMG		CG		CAMG		<i>i</i> CAMG	
	Its	T_c	Its	T_c	Its	T_c	Its	T_c	Its	T_c	Its	T_c
512	151	3.23E-2	7	1.54E-2	7	5.52E-3	249	5.43E-2	5	1.31E-2	5	4.58E-3
1024	225	9.41E-2	7	6.93E-2	8	1.63E-2	479	2.08E-1	5	6.97E-2	5	1.29E-2
2048	300	2.95E-1	7	2.86E-1	9	4.79E-2	920	9.19E-1	5	2.89E-1	5	3.75E-2
4096	385	6.99E-1	7	1.27E+0	9	1.38E-1	*	*	5	1.21E+0	5	1.10E-1

Table 11, 12 and 13 respectively give the results for cases $\tau = h$, $\tau = h^2$ and $\tau = 1/64$, which illustrate that CAMG and *i*CAMG both converge robustly with respect to mesh sizes and fractional

Table 12: Number of iterations and wall time for the case $\tau = h^2$.

M	$\alpha_0 = 0.9, \alpha_1 = 0.4, \beta = 0.3, \gamma = 0.8$						$\alpha_0 = 0.7, \alpha_1 = 0.5, \beta = 0.15, \gamma = 0.7$					
	CG		CAMG		<i>i</i> CAMG		CG		CAMG		<i>i</i> CAMG	
	<i>Its</i>	T_c	<i>Its</i>	T_c	<i>Its</i>	T_c	<i>Its</i>	T_c	<i>Its</i>	T_c	<i>Its</i>	T_c
512	8	1.62E-3	10	7.19E-3	8	1.12E-3	17	3.82E-3	7	1.39E-2	17	3.82E-3
1024	8	3.58E-3	8	3.29E-2	8	3.58E-3	17	7.01E-3	7	6.49E-2	17	7.01E-3
2048	8	8.01E-3	8	1.07E-1	8	8.81E-3	17	1.73E-2	7	2.62E-1	17	1.73E-2
4096	9	1.82E-2	9	4.70E-1	9	1.82E-2	17	3.29E-2	7	1.04E+0	17	3.29E-2

Table 13: Number of iterations and wall time for the case $\tau = 1/64$.

M	$\alpha_0 = 0.9, \alpha_1 = 0.4, \beta = 0.3, \gamma = 0.8$						$\alpha_0 = 0.7, \alpha_1 = 0.5, \beta = 0.15, \gamma = 0.95$					
	CG		CAMG		<i>i</i> CAMG		CG		CAMG		<i>i</i> CAMG	
	<i>Its</i>	T_c	<i>Its</i>	T_c	<i>Its</i>	T_c	<i>Its</i>	T_c	<i>Its</i>	T_c	<i>Its</i>	T_c
512	173	3.69E-2	7	1.65E-2	7	5.56E-3	250	5.38E-2	5	1.25E-2	4	3.88E-3
1024	301	1.26E-1	8	7.55E-2	7	1.55E-2	483	2.04E-1	5	5.65E-2	4	1.10E-2
2048	524	5.32E-1	8	3.10E-1	7	4.48E-2	933	9.37E-1	5	2.31E-1	4	3.07E-2
4096	908	1.66E+0	8	1.31E+0	7	1.25E-1	*	*	5	1.01E+0	4	8.71E-2

orders, while CG is only suitable for $\tau = h^2$ because of (23). *i*CAMG adaptively adjusts to be CG in such circumstance. Here our emphasis is on computational effort. The cost of *i*CAMG increases $\mathcal{O}(M \log M)$, yet CAMG bears $\mathcal{O}(M^2)$ to achieve convergence. Hence, *i*CAMG exhibits a significant advantage over CAMG, runs 9.2 and 11.0 times faster for $\tau = h$, 25.8 and 31.6 for $\tau = h^2$, 10.5 and 11.6 for $\tau = 1/64$ at the size of $M = 4096$.

5. Conclusion

Classical AMG is an $\mathcal{O}(M^2)$ solution process for SFDEs. We have proposed a lossless in robustness and adaptive variant with $\mathcal{O}(M \log M)$ algorithmic complexity and $\mathcal{O}(M)$ matrix-free storage, employed to solve the time-space FE discretization of one-dimensional MTFDEs. The approach relied on a number of theoretically proved characterizations and condition number estimation on the resulting matrix, an effective measure on the strength-of-connection tolerance and straightforward modifications to grid-transfer operators. Our numerical results verify the saturation error order of the discretization, well robustness and considerable advantages of the proposed solver over CG and classical AMG methods.

Acknowledgments

This work is under auspices of National Natural Science Foundation of China (11571293, 11601460, 11601462) and the General Project of Hunan Provincial Education Department of China (16C1540, 17C1527).

References

References

- [1] K. S. Miller and B. Ross, An introduction to the fractional calculus and fractional differential equations, Wiley (1993).
- [2] F. Liu, P. Zhuang, V. Anh, I. Turner, and K. Burrage, Stability and convergence of the difference methods for the space-time fractional advection-diffusion equation, *Appl. Math. Comput.* 191 (1) (2007), pp. 12-20.
- [3] G. H. Gao and Z. Z. Sun, A compact finite difference scheme for the fractional sub-diffusion equations, *J. Comput. Phys.* 230 (3) (2011), pp. 586-595.
- [4] X. N. Cao, J. L. Fu and H. Huang, Numerical method for the time fractional Fokker-Planck equation, *Adv. Appl. Math. Mech.* 4 (6) (2012), pp. 848-863.
- [5] H. Wang and T. S. Basu, A fast finite difference method for two-dimensional space-fractional diffusion equations, *SIAM J. Sci. Comput.* 34 (5) (2012), pp. A2444-A2458.
- [6] W. Yang, D. L. Wang and L. Yang, A stable numerical method for space fractional Landau-Lifshitz equations, *Appl. Math. Lett.* 61 (2016), pp. 149-155.
- [7] V. J. Ervin and J. P. Roop, Variational formulation for the stationary fractional advection dispersion equation, *Numer. Methods Partial Differ. Equ.* 22 (3) (2006), pp. 558-576.
- [8] H. Zhang, F. Liu and V. Anh, Galerkin finite element approximation of symmetric space-fractional partial differential equations, *Appl. Math. Comput.* 217 (6) (2010), pp. 2534-2545.
- [9] K. Burrage, N. Hale and D. Kay, An efficient implicit FEM scheme for fractional-in-space reaction-diffusion equations, *SIAM J. Sci. Comput.* 34 (4) (2012), pp. A2145-A2172.

- [10] W. P. Bu, Y. F. Tang and J. Y. Yang, Galerkin finite element method for two-dimensional Riesz space fractional diffusion equations, *J. Comput. Phys.* 276 (2014), pp. 26-38.
- [11] K. Mustapha, B. Abdallah and K. M. Furati, A discontinuous Petrov-Galerkin method for time-fractional diffusion equations, *SIAM J. Numer. Anal.* 52 (5) (2014), pp. 2512-2529.
- [12] L. B. Feng, P. Zhuang, F. Liu, I. Turner, and Y. T. Gu, Finite element method for space-time fractional diffusion equation, *Numer. Algor.* 72 (3) (2016), pp. 749-767.
- [13] W. P. Bu, A. G. Xiao and W. Zeng, Finite difference/finite element methods for distributed-order time fractional diffusion equations, *J. Sci. Comput.* 72 (1) (2017), pp. 422-441.
- [14] F. Liu, P. Zhuang, I. Turner, K. Burrage, and V. Anh, A new fractional finite volume method for solving the fractional diffusion equation, *Appl. Math. Model.* 38 (15-16) (2014), pp. 3871-3878.
- [15] Y. M. Lin and C. J. Xu, Finite difference/spectral approximations for the time-fractional diffusion equation, *J. Comput. Phys.* 225 (2) (2007), pp. 1533-1552.
- [16] M. Zayernouri, W. R. Cao, Z. Q. Zhang, and G. E. Karniadakis, Spectral and discontinuous spectral element methods for fractional delay equations, *SIAM J. Sci. Comput.* 36 (6) (2014), pp. B904-B929.
- [17] Y. Yang, Y. P. Chen and Y. Q. Huang, Spectral-collocation method for fractional Fredholm integro-differential equations, *J. Korean Math. Soc.* 51 (1) (2014), pp. 203-224.
- [18] Y. Yang, Jacobi spectral Galerkin methods for Volterra integral equations with weakly singular kernel, *Bull. Korean Math. Soc.* 53 (1) (2016), pp. 247-262.
- [19] R. Metzler and J. Klafter, The random walk's guide to anomalous diffusion: a fractional dynamics approach, *Phys. Rep.* 339 (2000), pp. 1-77.
- [20] S. Shen, F. Liu, V. Anh, and I. Turner, The fundamental solution and numerical solution of the Riesz fractional advection-dispersion equation, *IMA J. Appl. Math.* 73 (6) (2008), pp. 850-872.
- [21] Y. Y. Zheng, C. P. Li and Z. G. Zhao, A note on the finite element method for the space-fractional advection diffusion equation, *Comput. Math. Appl.* 59 (5) (2010), pp. 1718-1726.
- [22] M. M. Meerschaert and C. Tadjeran, Finite difference approximations for fractional advection-dispersion flow equations, *J. Comput. Appl. Math.* 172 (1) (2004), pp. 65-77.

- [23] A. H. Bhrawy and D. Baleanu, A spectral Legendre-Gauss-Lobatto collocation method for a
375 space-fractional advection diffusion equations with variable coefficients, *Rep. Math. Phys.* 72
(2) (2013), pp. 219-233.
- [24] H. Jiang, F. Liu, I. Turner, and K. Burrage, Analytical solutions for the multi-term time-space
Caputo-Riesz fractional advection-diffusion equations on a finite domain, *J. Math. Anal. Appl.*
389 (2) (2012), pp. 1117-1127.
- [25] H. Ye, F. Liu, V. Anh, and I. Turner, Maximum principle and numerical method for the
380 multi-term time-space Riesz-Caputo fractional differential equations, *Appl. Math. Comput.* 227
(2014), pp. 531-540.
- [26] W. P. Bu, X. T. Liu, Y. F. Tang, and J. Y. Yang, Finite element multigrid method for multi-
term time fractional advection diffusion equations, *Int. J. Model. Simul. Sci. Comput.* 6 (2015),
385 1540001.
- [27] C. Y. Gong, W. M. Bao, G. J. Tang, Y. W. Jiang, and J. Liu, Computational challenge of
fractional differential equations and the potential solutions: a survey, *Math. Probl. Eng.* 2015
(2015), 258265.
- [28] U. Trottenberg, C. W. Oosterlee and A. Schüller, *Multigrid*, Elsevier (2001).
- [29] C. S. Feng, S. Shu, J. Xu, and C. S. Zhang, Numerical study of geometric multigrid methods
390 on CPU-GPU heterogeneous computers, *Adv. Appl. Math. Mech.* 6 (1) (2014), pp. 1-23.
- [30] R. D. Falgout, S. Friedhoff, Tz. V. Kolev, S. P. Maclachlan, and J. B. Schroder, Parallel time
integration with multigrid, *SIAM J. Sci. Comput.* 36 (6) (2014), pp. C635-C661.
- [31] J. Xu and L. Zikatanov, Algebraic multigrid methods, *Acta Numer.* 26 (2017), pp. 591-721.
- [32] H. K. Pang and H. W. Sun, Multigrid method for fractional diffusion equations, *J. Comput.*
395 *Phys.* 231 (2012), pp. 693-703.
- [33] Z. Q. Zhou and H. Y. Wu, Finite element multigrid method for the boundary value problem of
fractional advection dispersion equation, *J. Appl. Math.* 2013 (2013), 385463.
- [34] Y. J. Jiang and X. J. Xu, Multigrid methods for space fractional partial differential equations,
400 *J. Comput. Phys.* 302 (2015), pp. 374-392.

- [35] L. Chen, R. H. Nochetto, E. Otárola, and A. J. Salgado, Multilevel methods for nonuniformly elliptic operators and fractional diffusion, *Math. Comput.* 85 (302) (2016), pp. 2583-2607.
- [36] X. Zhao, X. Z. Hu, W. Cai, and G. E. Karniadakis, Adaptive finite element method for fractional differential equations using hierarchical matrices, *Comput. Methods Appl. Mech. Engrg.* 325 (2017), pp. 56-76.
- 405 [37] M. H. Chen and W. H. Deng, Convergence proof for the multigrid method of the nonlocal model, arXiv: 1605.05481.
- [38] X. Q. Yue, W. P. Bu, S. Shu, M. H. Liu, and S. Wang, Fully finite element adaptive algebraic multigrid method for time-space Caputo-Riesz fractional diffusion equations, arXiv: 1707.08345.
- 410 [39] Y. Saad, *Iterative methods for sparse linear systems*, SIAM (2003).
- [40] J. Xu and L. Zikatanov, Algebraic multigrid methods, *Acta Numer.* 26 (2017), pp. 591-721.
- [41] V. E. Henson and U. M. Yang, BoomerAMG: A parallel algebraic multigrid solver and preconditioner, *Appl. Numer. Math.* 41 (2002), pp. 155-177.
- [42] M. Naumov et al., AmgX: A library for GPU accelerated algebraic multigrid and preconditioned iterative methods, *SIAM J. Sci. Comput.* 37 (5) (2015), pp. S602-S626.
- 415